

Stabilization of Colloidal Suspensions by Means of Highly Charged Nanoparticles

Jiwen Liu and Erik Luijten*

*Department of Materials Science and Engineering and Frederick Seitz Materials Research Laboratory,
University of Illinois at Urbana-Champaign, 1304 West Green Street, Urbana, Illinois 61801, USA*

(Received 22 September 2004; published 7 December 2004)

We employ a novel Monte Carlo simulation scheme to elucidate the stabilization of neutral colloidal microspheres by means of highly charged nanoparticles [V. Tohver *et al.*, Proc. Natl. Acad. Sci. U.S.A. **98**, 8950 (2001)]. In accordance with the experimental observations, we find that small nanoparticle concentrations induce an effective repulsion that prevents gelation caused by the intrinsic van der Waals attraction between colloids. Higher nanoparticle concentrations induce an attractive potential which is, however, qualitatively different from the regular depletion attraction. We also show how colloid-nanoparticle size asymmetry and nanoparticle charge can be used to manipulate the effective interactions.

DOI: 10.1103/PhysRevLett.93.247802

PACS numbers: 82.70.Dd, 61.20.Ja

Colloidal particles find widespread application as precursors for nanostructured materials, including advanced coatings, drug carriers, and colloidal crystals. These materials are frequently fabricated from the liquid phase via hierarchical self-assembly processes that are governed by the interactions of the particles, their shape, and their size. The understanding and prediction of phase behavior and stability of a suspension relies on a fundamental knowledge of the *effective* forces between colloids [1], which arise from a combination of direct interactions and indirect interactions mediated by the solvent and by other solute particles. Traditional methods to stabilize a suspension typically involve tuning of the effective interactions through charged groups or through grafting short polymer chains onto the colloidal surface. These mechanisms, however, pose serious problems in certain situations, such as the fabrication of close-packed colloidal crystals, where they cause an increase in the lattice spacing of the sedimented colloids and thus lead to cracking of the crystal upon drying.

It is, therefore, of great fundamental and practical interest that an alternative stabilization strategy has emerged [2,3]. In these experiments, the addition of very small concentrations of charged zirconia nanoparticles was found to prevent the aggregation of near-neutral silica microspheres in aqueous suspension. Upon further increase of the zirconia concentration, microsphere aggregation was recovered, leading to a “window of stability.” Lewis and coworkers [2] ascribe the initial colloidal stabilization to the formation of a nonadsorbing “halo” of zirconia particles around the silica colloids, arising from the strong electrostatic repulsion between nanoparticles. However, while consistent with zeta-potential measurements that confirm a weak accumulation of nanoparticles near the colloidal surface, such halo formation is at variance with the observation of stabilization at zirconia volume fractions below 10^{-3} , where the average nanoparticle separation is approximately 40 nm, significantly larger than the electrostatic screening length $\kappa^{-1} \approx 2$ nm

[3]. On the other hand, the reentrant gelation is attributed to the regular depletion attraction induced by the nanoparticles [4]. This is a potentially contentious argument as well, as it has been demonstrated that the depletion effect can be substantially modified by nonadditivity effects [5–7] which, in this case, would result from the electrostatic repulsions.

Unfortunately, theoretical and computational approaches experience severe difficulties in the treatment of this system. Analytical methods commonly incorporate fluctuation and correlation effects only in an approximate manner. While simulations can explicitly account for these effects, inherent limitations in most computational methodologies greatly restrict the range of accessible size ratios in multicomponent mixtures. In this Letter, we overcome this problem by exploiting a novel, highly-efficient Monte Carlo scheme [8], which permits the explicit inclusion of interacting species of vastly different sizes. Thus, we are able to determine the distribution of nanoparticles and the colloidal potential of mean force as a function of nanoparticle concentration. Our findings constitute the first *quantitative* confirmation of the experimental observations and clarify the underlying physical mechanism of the stabilization. In addition, we provide explicit predictions for the role of two crucial parameters, the magnitude of the nanoparticle charge and the colloid-nanoparticle size asymmetry.

It is the purpose of our calculation to determine the effective pair potential between colloidal particles induced by the nanoparticles. This effective interaction is independent of the intrinsic van der Waals attraction. If sufficiently repulsive, it can counteract the latter and, thus, stabilize the suspension. Both species are modeled as hard spheres with diameter σ_{micro} and σ_{nano} , respectively. The aqueous environment (water and screening ions) is represented as a homogeneous medium. In addition, we take into account the electrostatic double-layer interactions by means of the well-known Hogg-Healy-Fuerstenau (HHF) formula [9,10]. For two nanoparticles

at a surface separation D , this equation, under constant-potential conditions, reduces to [11]

$$\begin{aligned} V_{\text{nano-nano}} &= \varepsilon_0 \varepsilon_r \pi \sigma_{\text{nano}} \Psi_{\text{nano}}^2 \ln[1 + \exp(-\kappa D)] \\ &\approx \varepsilon_0 \varepsilon_r \pi \sigma_{\text{nano}} \Psi_{\text{nano}}^2 \exp(-\kappa D), \end{aligned} \quad (1)$$

where the approximation is valid for $\kappa D \gg 1$. Ψ_{nano} is the zirconia zeta-potential, ε_0 the vacuum permittivity, and $\varepsilon_r = 80$ the dielectric constant of water. Since the silica spheres are negligibly charged, we ignore their electrostatic interaction. However, an electrostatic double-layer interaction arises between the microspheres and the nanoparticles, which, for large size asymmetry $\alpha \equiv \sigma_{\text{micro}}/\sigma_{\text{nano}} \gg 1$ is described by [9]

$$\begin{aligned} V_{\text{micro-nano}} &= \frac{1}{2} \varepsilon_0 \varepsilon_r \pi \sigma_{\text{nano}} \Psi_{\text{nano}}^2 \ln[1 - \exp(-2\kappa D)] \\ &\approx -\frac{1}{2} \varepsilon_0 \varepsilon_r \pi \sigma_{\text{nano}} \Psi_{\text{nano}}^2 \exp(-2\kappa D), \end{aligned} \quad (2)$$

where the approximation is again valid for $\kappa D \gg 1$. While charge-regulating boundary conditions are even more appropriate than constant-potential boundary conditions for the interactions (1) and (2), both conditions have been found to lead to comparable results [12]. In particular, the former can also yield an attraction between neutral and charged surfaces [13]. Indeed, whereas the presence of a microsphere-nanoparticle attraction is not considered explicitly in Ref. [2], both the supernatant measurements and the dynamic nature of the zeta-potential measurement (which implies a cooperative movement of colloids and nanoparticles) indicate a certain degree of microsphere-nanoparticle association. It must be emphasized, however, that this attractive interaction by itself does *not* reduce the problem to a standard case of electrostatic stabilization resulting from an effective charge build-up on the colloids. Instead, as is shown below, the resulting halo is dynamic in nature and leads to effective interactions that are either attractive, repulsive, or oscillatory, depending on nanoparticle concentration.

The presence of a short-range attraction is indeed confirmed in Fig. 1, which provides a quantitative comparison of the Monte Carlo simulations and the supernatant measurements. The adsorption of nanoparticles with diameter $\sigma_{\text{nano}} = 6$ nm around a microsphere with diameter $\sigma_{\text{micro}} = 0.6 \mu\text{m}$ is determined as a function of nanoparticle concentration, at fixed volume fraction $\phi_{\text{micro}} = 0.1$. In order to account for colloidal many-body effects and to handle the extreme size asymmetry ($\alpha = 100$), we use the generalized geometric cluster algorithm [8] for a system containing 50 colloids and up to 5×10^6 nanoparticles. In view of the small screening length and the presence of short-range hydration forces, we employ the approximate expressions in Eqs. (1) and (2) [14]. The amount of adsorbed nanoparticles, which form a layer with an approximate thickness σ_{nano} , is determined from the radial distribution function integrated from contact to its first minimum. While the

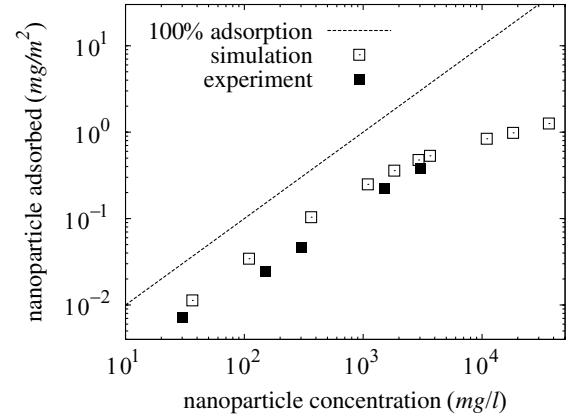


FIG. 1. Nanoparticle adsorption per colloidal microsphere as a function of zirconia nanoparticle concentration, at fixed $\phi_{\text{micro}} = 0.1$. The empty squares represent the simulation results and the filled squares the experimental data [2]. $\phi_{\text{nano}} = 10^{-3}$ corresponds to a concentration of 3650 mg/l.

Monte Carlo data to some extent overestimate the adsorption, both data sets exhibit a linear dependence on ϕ_{nano} and a degree of adsorption that is far below 100%. The overestimation is compatible with the high zeta-potential $\Psi_{\text{nano}} = 70$ mV, somewhat above the regime of validity of the Debye-Hückel approximation employed in the HHF equations [15]. At volume fractions above 10^{-3} the mutual repulsion between the charged nanoparticles causes the adsorption to level off.

Having established that the HHF equations model the experimental situation relatively accurately, we proceed to determine the effective (induced) colloidal interaction as a function of nanoparticle volume fraction. In the infinite dilution limit the potential of mean force follows from the colloidal pair correlation function, $V_{\text{eff}} = -k_B T \ln g(r)$. The simulations employ a cubic box with $\phi_{\text{micro}} = 0.002$ [16]. As shown in Fig. 2(a), at very low $\phi_{\text{nano}} = 7 \times 10^{-4}$ a strong attraction exists at a separation σ_{nano} , accompanied by a repulsive barrier of approximately $5k_B T$. The potential well arises from nanoparticles acting as “linkers” between two colloidal microspheres. However, upon increase of ϕ_{nano} to 10^{-3} the bridging attraction rapidly turns into a strong repulsion that extends over several nanoparticle diameters. Since the direct van der Waals interaction has a strength of only approximately $-1k_B T$ at a surface separation σ_{nano} [3], the total interaction exhibits a barrier. This repulsive barrier, which continues to increase with ϕ_{nano} , is sufficiently strong to prevent gelation and thus leads to (kinetic) stabilization of the suspension. The corresponding threshold agrees remarkably well with the experimentally observed gel-fluid transition near $\phi_{\text{nano}} = 5 \times 10^{-4}$ [2].

If the nanoparticle volume fraction is raised further, however, an attractive well arises for $D \approx 4\sigma_{\text{nano}}$ [Fig. 2(b)]. As shown in the inset, the attraction strength grows as ϕ_{nano}^2 . At $\phi_{\text{nano}} = 10^{-2}$ it reaches nearly $-3k_B T$,

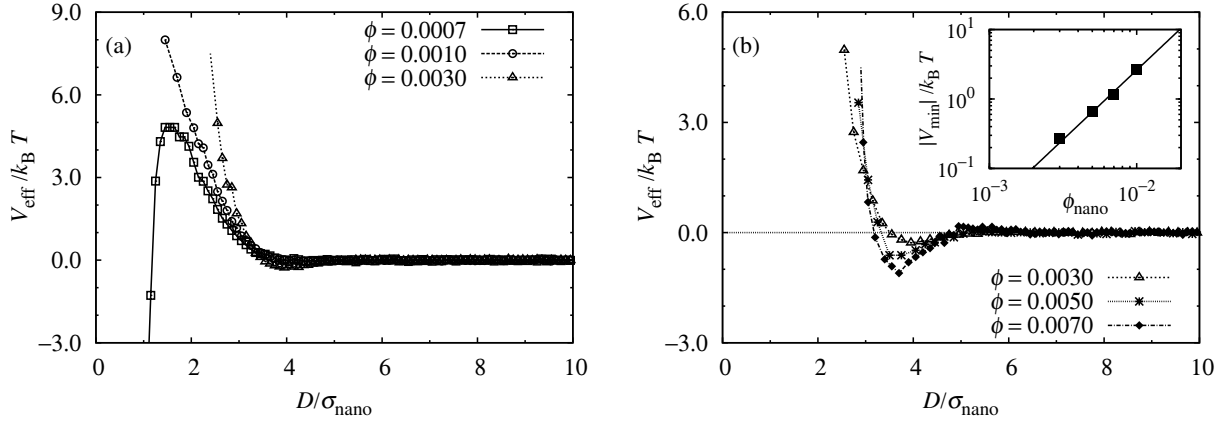


FIG. 2. Effective potential $V_{\text{eff}}/k_B T$ between a pair of colloidal microspheres as a function of surface-to-surface separation D . (a) At low nanoparticle volume fractions a bridging attraction is observed, which rapidly turns into a strong effective repulsion. (b) At higher volume fractions an attractive minimum develops, with a strength that grows *quadratically* with ϕ_{nano} (inset).

which is estimated to be sufficient to induce gelation. Again, this packing fraction agrees quite well with the experimentally observed reentrant gelation for $\phi_{\text{nano}} \approx 5 \times 10^{-3}$. The quadratic growth of the attraction strength with ϕ_{nano} indicates that this is not a regular depletion attraction, which has a linear concentration dependence [4]. Indeed, examination of configurations shows only limited nanoparticle depletion between colloidal pairs at $D \approx 4\sigma_{\text{nano}}$.

In order to gain a microscopic understanding of the effective potentials we study the distribution of nanoparticles around a pair of colloids, for various separations of the colloidal particles. For clarity in the graphs, we employ a smaller size ratio $\alpha = 40$ (i.e., $\sigma_{\text{micro}} = 0.24 \mu\text{m}$) with $\phi_{\text{nano}} = 0.003$, for which the effective interaction is strongly repulsive [cf. Figure 4(a) for $\phi_{\text{nano}} = 0.001$]. At a surface separation $D \geq 5\sigma_{\text{nano}}$ [Fig. 3(a)] the halos around both colloids are uniform, in agreement with a negligible effective interaction. If the colloids are forced closer together, the mutual repulsion between the nanoparticles leads to a redistribution of particles in the halo. At a separation $D = 1.8\sigma_{\text{nano}}$ [Fig. 3(b)] most nanoparticles have been expelled from the gap region and a depletion zone appears. While reminiscent of the depletion effect in hard-sphere mixtures [4], the effective colloidal interaction in this case is strongly *repulsive* rather than attractive. This indicates that the energy penalty resulting from nanoparticle rearrangements dominates over depletionlike entropic effects.

The “haloing” stabilization mechanism clearly relies on rather generic features and hence may become of considerable practical importance. Since applications hinge on an understanding of the role of size and charge asymmetry, we have investigated a variety of parameter combinations. Figure 4(a) displays the repulsion resulting from a fixed volume fraction $\phi_{\text{nano}} = 0.001$ for colloids of diameter $0.60 \mu\text{m}$, $0.36 \mu\text{m}$, and $0.24 \mu\text{m}$ (size ratio $\alpha = 100, 60$, and 40 , respectively). Consistent with experimental observation [2], the effective colloidal repul-

sion increases with α . As shown in the inset, the dependence on size asymmetry is almost perfectly linear. The role of the nanoparticle *charge* is certainly complicated, as it affects both halo formation and the halo-halo interaction. Indeed, if the nanoparticle distribution around a pair of colloids at surface separation D is denoted by $\rho(\mathbf{r}'; D)$, where \mathbf{r}' is measured with respect to the first colloid, then the effective force on that colloid is

$$\mathbf{F}(D) = - \int \rho(\mathbf{r}'; D) \frac{\partial}{\partial \mathbf{r}'} V_{\text{micro-nano}}(r') d\mathbf{r}'. \quad (3)$$

The nanoparticle charge will affect both $\rho(\mathbf{r}'; D)$ and $V_{\text{micro-nano}}$. In the absence of experimental data, we have performed simulations for the $\alpha = 100$ case with a lower nanoparticle surface potential, $\Psi_{\text{nano}} = 50 \text{ mV}$ [Fig. 4(b)]. The effective interactions are found to be similar to those for higher surface potentials, with a comparable dependence on ϕ_{nano} , but almost ten times larger volume fractions are needed to achieve the same effective colloidal repulsion. This emphasizes the important role of the nanoparticle charge. Finally, we have performed control simulations in which the colloid-

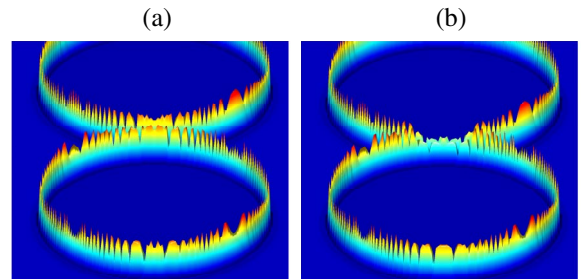


FIG. 3 (color online). Nanoparticle density distribution around two colloidal particles at a surface-to-surface distance D . (a) At larger separations ($D = 5.0\sigma_{\text{nano}}$) the halos around each colloid are uniform. (b) Upon closer approach ($D = 1.8\sigma_{\text{nano}}$), where there is a strong colloidal repulsion, a *depletion* of nanoparticles in the gap region is observed.

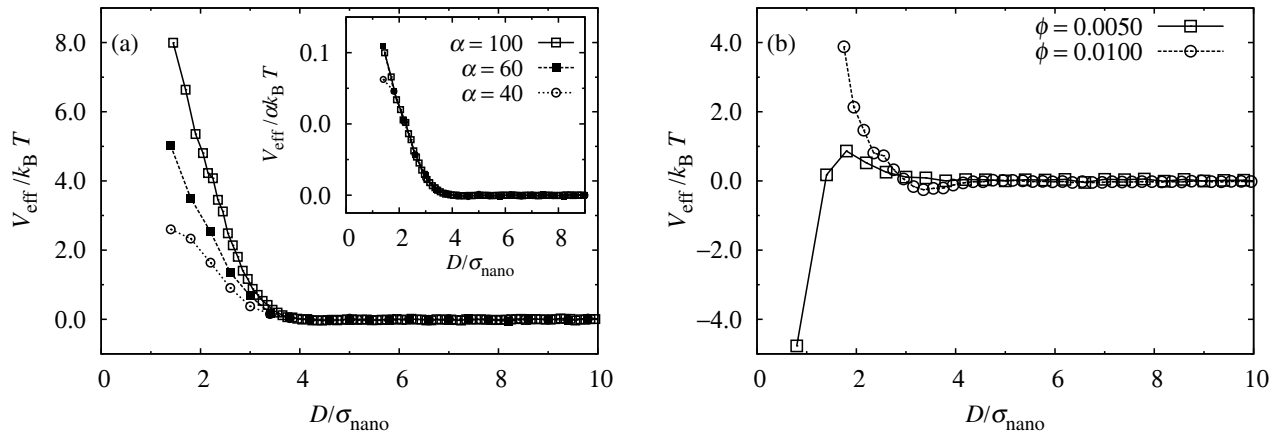


FIG. 4. (a) Effect of nanoparticle-colloid size asymmetry α on the effective colloidal interactions. At fixed nanoparticle size and volume fraction $\phi_{\text{nano}} = 0.001$, the repulsion increases with colloid size. As shown in the inset, the dependence is virtually perfectly linear. (b) Effect of nanoparticle charge. All parameters are identical to those in Fig. 2, except for the nanoparticle surface potential, which has been lowered from 70 mV to 50 mV. As a result, much larger nanoparticle volume fractions are required to achieve an appreciable colloidal repulsion.

nanoparticle attraction is omitted. Neither the observed adsorption (Fig. 1) nor the effective repulsions (Fig. 2) can be reproduced unless the nanoparticle concentrations are *much* higher than in the experiment or the nanoparticle repulsion has a much longer range, which in turn would be incompatible with the actual screening length $\kappa^{-1} \approx \sigma_{\text{nano}}/3$ [3].

In summary, the mechanism for colloidal stabilization through nanoparticle haloing [2] has been clarified by means of direct simulation. The geometric cluster algorithm, which provides an acceleration of many orders of magnitude [8], has been indispensable for this: At a nanoparticle volume fraction $\phi_{\text{nano}} = 0.007$ the calculation involves 7×10^6 nanoparticles, requiring a simulation of $\mathcal{O}(10^4)$ hours. We have shown that an induced colloid-nanoparticle attraction contributes to the effective repulsion, but that it by no means reduces the situation to simple steric or Coulombic stabilization. Haloing stabilization occurs over a window of nanoparticle concentrations, bracketed by two dissimilar gel phases, neither of which is a regular depletion gel. Our calculations indicate that the effective colloidal interactions also sensitively depend on nanoparticle charge and colloid-nanoparticle size asymmetry, so that the haloing mechanism indeed opens up a variety of opportunities to tailor materials properties.

We gratefully acknowledge stimulating discussions with Jennifer Lewis and Ken Schweizer. This material is based upon work supported by the U.S. Department of Energy, Division of Materials Sciences under Grant No. DEFG02-91ER45439, through the Frederick Seitz Materials Research Laboratory at the University of Illinois at Urbana-Champaign and by the National Science Foundation under Grants No. DMR-0346914 and CTS-0120978.

Note added:—Upon completion of this work we became aware of a study by Karanikas and Louis, who

use different techniques, but arrive at similar conclusions.

*Corresponding author.

Email address: luitjen@uiuc.edu

- [1] W. B. Russell, D. A. Saville, and W. R. Schowalter, *Colloidal Dispersions* (Cambridge University Press, Cambridge, England, 1989).
- [2] V. Tohver, J. E. Smay, A. Braem, P. V. Braun, and J. A. Lewis, Proc. Natl. Acad. Sci. U.S.A. **98**, 8950 (2001).
- [3] V. Tohver, A. Chan, O. Sakurada, and J. A. Lewis, Langmuir **17**, 8414 (2001).
- [4] S. Asakura and F. Oosawa, J. Chem. Phys. **22**, 1255 (1954).
- [5] J. M. Méndez-Alcaraz and R. Klein, Phys. Rev. E **61**, 4095 (2000).
- [6] R. Roth, R. Evans, and A. A. Louis, Phys. Rev. E **64**, 051202 (2001).
- [7] A. A. Louis, E. Allahyarov, H. Löwen, and R. Roth, Phys. Rev. E **65**, 061407 (2002).
- [8] J. Liu and E. Luitjen, Phys. Rev. Lett. **92**, 035504 (2004).
- [9] R. Hogg, T. W. Healy, and D. W. Fuerstenau, Trans. Faraday Soc. **62**, 1638 (1966).
- [10] J. E. Sader, S. L. Carnie, and D. Y. C. Chan, J. Colloid Interface Sci. **171**, 46 (1995).
- [11] R. J. Hunter, *Foundations of Colloid Science* (Oxford University Press, Oxford, England, 2001), 2nd ed.
- [12] S. H. Behrens and M. Borkovec, Phys. Rev. E **60**, 7040 (1999).
- [13] P. M. Biesheuvel, J. Colloid Interface Sci. **275**, 514 (2004).
- [14] To account for the hydration shell of the zirconia nanoparticles, σ_{nano} is replaced by $\sigma'_{\text{nano}} = \sigma_{\text{nano}} + 1.5$ nm solely in Eq. (1).
- [15] Explicit solution of the nonlinear Poisson-Boltzmann equation yields an electrostatic attraction with a contact value approximately 25% lower than Eq. (2) [10].
- [16] We have verified that the results remain unchanged upon further decrease of the colloid volume fraction.